Evaluation of Common Complications Following Tetralogy of Fallot Surgical Repair by Magnetic Resonance Imaging

Zainab Ahmad Ramadan

M.D of Diagnostic Radiology Mansoura University Faculty of Medicine EGYPT, zainabahmed87@mans.edu.eg

Mohamed Salah Ayyad

M.sc of Diagnostic Radiology Mansoura University Faculty of Medicine EGYPT

Evaluation of Common Complications Following Tetralogy of Fallot Surgical Repair by Magnetic Resonance Imaging

Evaluation of Common Complications Following Tetralogy of Fallot Surgical Repair by Magnetic Resonance Imaging

Zainab A. Ramadan*, Mohamed S. Ayyad

Department of Diagnostic Radiology, Faculty of Medicine, Mansoura University, Mansoura, Egypt

Abstract

Background: The operative procedures for correction of tetralogy of Fallot (TOF) concentrate on the impact of pulmonary valve regurgitation (PR) on the function of the right ventricle (RV) pointing to alleviating right ventricle outflow tract (RVOT) narrowing, and minimizing the PR degree at the same time, closing ventricular septal defect (VSD). Various complications could be encountered after TOF repair such as PR, dilated RV with/without impaired function, RVOT residual obstruction/dilatation, residual VSD, tricuspid regurge (TR), aortic root dilatation with/without regurge, and significant difference in differential pulmonary flow.

Objective: To address the most common complications that could be encountered following TOF surgical repair, the role of cardiac magnetic resonance imaging in evaluation of these complications, and summarize them as a checklist for reporting postoperative cases.

Methods: A retrospective study involved 116 patients, their ages ranging from 2 to 18 years (mean ± standard deviation (SD) = 8.1 ± 4.5) from March 2021 to May 2023, evaluated for possible complications following TOF operative repair by MRI.

Results: In total, 105 patients had dilated RV. About 31 patients had impaired function. All patients had PR. In total, 12 had severe TR and 18 had aortic regurgitation. About 18 had residual VSD. In total, 7 had residual RVOT stenosis and 5 had aneurysmally dilated RVOT. About 39 patients had significant differences in differential pulmonary flow.

Conclusions: MRI is critical for evaluation of post-TOF repair patients and possible complications. Cardiac magnetic resonance imaging is accurate in quantifying PR, RV size and function, and evaluating other possible important complications related to RVOT, pulmonary arterial diameters and differential flow, and VSD closure and left ventricle function and size as well.

Keywords: Cardiac magnetic resonance imaging, Complications, Pulmonary valve regurgitation, Right ventricle outflow tract, Tetralogy of fallot operative repair

1. Introduction

Echocardiography is the mainstay of evaluation of tetralogy of Fallot (TOF) before and after surgical correction, as it provides worthy data about the cardiac chambers, valves, and hemodynamic parameters like predicted pulmonary and right ventricle (RV) pressures. It is also universally accessible, transportable, safe, and reproducible (Woodard *et al.*, 2017).

Preoperatively, computed tomography and cardiac magnetic resonance imaging (CMRI) were reserved for complex anatomy for better delineation of fine details (Renella *et al.*, 2010). Cardiac MRI is of extreme benefit for TOF evaluation principally after surgery (Schicchi *et al.*, 2016).

Cardiac MRI does not utilize ionizing radiation as computed tomography, and hence can be safely repeated. It can be achieved with numerous planes and images irrespective of the window of imaging or

* Corresponding author. Elgomhoria St., 35516, Mansoura, Egypt.
E-mail address: zainabahmed87@mans.edu.eg (Z.A. Ramadan).

patients' body configuration, which is a drawback of transthoracic echocardiography. Unlike two-dimensional (2D) echocardiography that is predominantly qualitatively used, CMRI gives valuable, accurate, quantitative, and objective measurements of the RV function and size, valvular regurge, differential pulmonic arterial flow, and delineation of myocardial scarring, all these data are remarkably critical in lifelong monitoring of TOF (Valente *et al.*, 2014).

'Bright blood' sequences, as steady-state free precession (SSFP) cine or gradient echo sequences, could detect flow jets in intracardiac shunts, valvular insufficiency, or stenosis. These sequences could also be utilized in volumetric coverage to measure RV and left ventricle (LV) volumes and function with outstanding accuracy (Haggerty *et al.*, 2017).

Phase-contrast sequences demonstrate direction and permit quantification of flow volume as well, thus giving an opportunity to identify intra- or extra-cardiac shunts, pressure gradients through obstructive lesions, and regurgitation fractions (RF) through incompetent valves (Geva, 2014).

Pulmonary regurgitation after TOF repair is very common with more than 80% of patients getting PR that finally leads to RV dilatation and dysfunction. Pulmonary arterial evaluation is important as well. The incidence of moderate-to-marked tricuspid regurgitation (TR) is about 10%. It is commonly functional secondary to progressive RV dilatation (Kalyan *et al.*, 2021).

Aortic root dilatation with or without no aortic insufficiency does not have uncommon incidence and may necessitate aortic valve and/or root operation if the dilatation is more than 5.5 cm. This is more common in adults than pediatrics. So, continuous monitoring of the aortic root and possible aortic regurgitation (AR) after TOF repair is advised (Kalyan *et al.*, 2021).

Residual right ventricle outflow tract (RVOT) obstruction can persist after initial repair because of hypertrophied muscle in the subvalvular region, hypoplastic annulus, or stenotic pulmonary valve. Mild narrowing is commonly well-accommodated, but significant obstruction may indicate intervention or even redo operation (Mercer-Rosa *et al.*, 2012).

Right ventricular outflow tract dilatation and aneurysms usually occur after the repair of TOF. CMRI is usually a better imaging modality for RVOT aneurysm. It is also very beneficial to describe RV structural and functional changes (Dahiya *et al.*, 2022).

For residual ventricular septal defect (VSD), despite being rare, immediate intervention will be required in physiologically significant VSDs. Routine monitoring will be needed to detect changes in size and shunt. Echocardiography is enough to detect most VSDs yet, they are also accurately detected with CMR imaging, and the shunt could be quantified. Shunting across small VSDs appears as a signal void jet on SSFP cine images (Kalyan *et al.*, 2021).

On detection of branch pulmonary artery stenosis, the diameters of the major pulmonary arteries are not an enough indicator of pulmonary blood flow to each lung. Phase-contrast MRI permits direct quantification of pulmonary blood flow to each lung (Kalyan *et al.*, 2021). The average (within normal range) blood flow distribution is 45% to the left lung and 55% to the right lung (Hysinger *et al.*, 2022).

2. Aim

To address the most common complications that could be encountered following TOF surgical repair, the role of cardiac MRI in the evaluation of these complications, and summarize them as a checklist for reporting postoperative cases.

3. Patients and methods

3.1. Patients

The study was approved by the Institutional Research Board (code number: R.23.07.2272) and informed consent was waived because of the retrospective nature of the study.

This was a retrospective study that involved 116 patients with their ages ranging from two to eighteen years (mean $\pm$ standard deviation (SD) = 8.1 $\pm$ 4.5). It was done at magnetic resonance imaging units of our Department of Radiology, over a period from March 2021 to May 2023. The patients were referred for evaluation as post-TOF definitive surgical correction routine monitoring.

3.2. Methods

All patients in the study underwent CMR imaging of the heart and related proximal great vessels.

3.3. Technique of cardiac MRI

Infants and noncooperative young children were sedated before MRI, while older children who could understand and obey instructions were not sedated. CMRI was done on (Ingenia 1.5 T; A Philips, Medical Systems, Best, the Netherlands) a superconducting magnet for all patients. Acquisition of all

data was retrospectively ECG-gated. The data were stocked in Digital Imaging and Communication in Medicine (DICOM) form for processing.

These stored data were then shifted to the workstation (extended MR workspace 2.6.3.5, Philips Medical Systems, Nederland B.V.).

3.4. Image acquisition and parameters

(1) Interactive images and localizers through the chest (TE; 1.4, TR; 2.8, FOV; 450 × 450 x 145, matrix; 224 × 256 x 10, voxel; 2.01 × 1.76 × 10).
(2) Dynamic interpretation in two planes, one is determined by the axial view and the other must be perpendicular to the first one. The structures to be evaluated involve RVOT, pulmonary arteries, VSD, and ascending aorta.
(3) SSFP cine sequences in the following views:
  (a) Axial (TR; 2.7, TE: 1.36, FOV; 180 × 180 x 88, matrix; 108 × 96 x 11, voxel; 1.7 × 1.7 × 8), four chambers (4-CH) [TR; 2.3, TE; 1.15, FOV; 180 × 180 x 72, matrix: 108 × 96 x 9, voxel; 1.7 × 1.7 × 8].
  (b) Short axis [SA] (TR; 2.18, TE; 1.09, FOV; 170 × 170 x 119, matrix; 100 × 78 x 17, voxel; 1.7 × 1.7 × 7).
  (c) Coronal (TE; 1.3, TR; 2.6, FOV; 180 × 180 x 84, matrix; 108 × 102 x 17, voxel; 1.7 × 1.7 × 7) SSFP cine involving the heart and proximal-related great vessels.
  (d) RVOT (TR; 2.94, TE; 1.47, FOV; 180 × 180 x 24, matrix; 104 × 104 x 3, voxel; 1.7 × 1.7 × 8).
  (e) Left ventricle outflow tract (LVOT) (TR; 2.8, TE; 1.4, FOV; 180 × 180 x 24, matrix; 108 × 96 x 3, voxel; 1.7 × 1.7 × 8) and three chambers (3-CH) of the LV, left atrium (LA), aortic valve, and aortic root (TR; 2.91, TE; 1.3, FOV; 180 × 180 x 24, matrix; 108 × 104 x 3, voxel; 1.7 × 1.7 × 8).
(4) Phase-contrast cine for main, right, and left pulmonary arteries (MPA, RPA, and LPA) and the ascending aorta (TR; 4.71, TE; 2.98, FOV; 300 × 248, matrix; 160 × 248, voxel; 1.9 × 1.9 × 8).

3.5. Images analysis

Cardiac MRI studies were analyzed by consultants' radiologists with an average of 8 years of cardiac imaging experience.

Cardiac MRI enabled us to interpret the anatomical details of the heart and proximal-related great vessels by SSFP cine sequence in the 3,4 CH, axial, coronal, SA, RVOT, and LVOT orientations.

Right ventricular volumes and functional interpretation was done using multislice SSFP cine images. A stack of sequential axial images was obtained from the cardiac apex to the base during end diastole and end systole for each slice location. End-systolic and end-diastolic volumes were estimated by summing up all slices, then calculation of ejection fraction and stroke volume was done. Left ventricular volumes and functional interpretation was done in a similar manner using a stack of sequential SA images.

Volumes of flow through the aorta, main, right, and left pulmonary arteries were measured using phase velocity maps. The region of interest was traced along the contour of the vessel lumen to determine the vessel area frame after frame and then calculation of the total forward, regurgitant and stroke volumes, and RF was done.

The regurgitant volume of tricuspid regurge was calculated by subtracting the pulmonary total forward flow volume from the RV stroke volume and the resulting volume divided by the RV stroke volume and multiplied by 100 to get the regurgitation fraction.

Volumes and diameters were determined as average, dilated, or small-sized (stenotic) according to calculation of body surface area and correlation of measurements to Z score where Z scores of 2 or more or −2 or less were considered significant (Buechel et al., 2009; Cantinotti et al., 2017).

3.6. Statistical analysis

(1) The data description was done as mean ± SD for continuous variables when normally distributed and as median and range when non-normally distributed.
(2) Categorical data were described using numbers and percentages, and median (minimum and maximum).

4. Results

This study involved 116 patients with variable post-TOF repair complications (Fig. 1). The ages' range was from 2 to 18 years (mean age±SD = 8.1 ± 4.5), 62 (53.4%) patients were boys (males), and 54 (46.6%) patients were girls (females) Table 1.

4.1. Right ventricle

The size of the right ventricle was measured for all patients by end-diastolic volume index (EDV divided by body surface area): 105 (90.5%) patients had dilated RV, while nine (7.8%) patients had
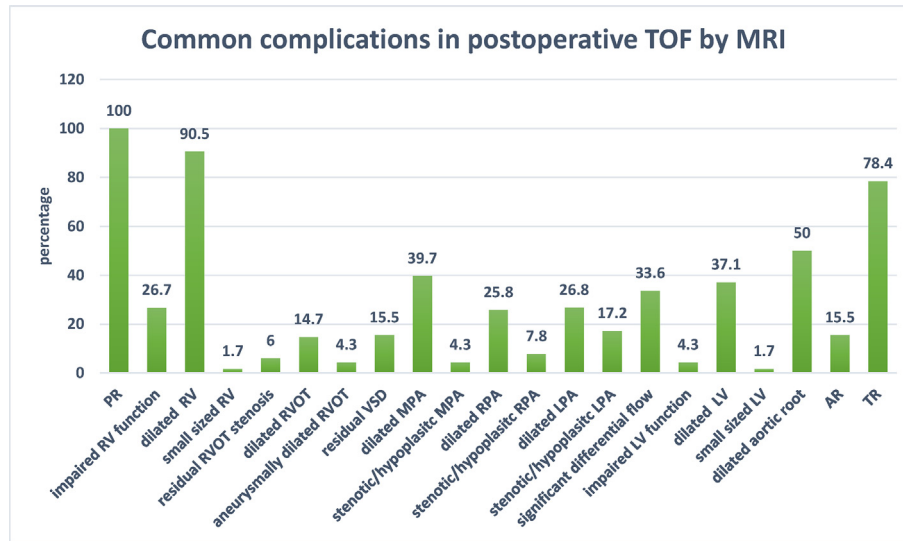
Fig. 1. Descriptive statistics of complications among the studied cases by MRI.

Table 1. Left ventricle and right ventricle sizes and function by magnetic resonance imaging.

Left ventricle	N = 116 (%)	Right ventricle	N = 116 (%)
EDVI		EDVI	
Mean ± SD	81.2 ± 22.34	Mean ± SD	148 ± 55.3
Median	79 (21−164)	Median	142 (30−466)
(minimum−maximum)		(minimum−maximum)	
EDVI*		Size	
Normal	71 (61.2)	Normal	9 (7.8)
Dilated	43 (37.1)	Dilated	105 (90.5)
Small-sized	2 (1.7)	Small-sized	2 (1.7)
Function		Function	
Persevered	111 (95.7)	Persevered	85 (73.3)
Impaired	5 (4.3)	Impaired	31 (26.7)
EF**		EF	
Median	64 (29−85)	Median	54.5 (20−73)
(minimum−maximum)		(minimum−maximum)	
Mean ± SD	64.1 ± 8.1	Mean ± SD	54.5 ± 8.4

* EDVI: end-diastolic volume index.
** EF: ejection fraction.

average RV size and two (1.7%) patients had small-sized RV (Table 1).

The right ventricular function was evaluated based on calculation of ejection fraction. In total, 85 (73.3%) patients had preserved function, while 31 (26.7%) patients had impaired function (Table 1).

4.2. Left ventricle

Seventy-one (61.2%) patients had average LV size, while 43 (37.1%) patients had dilated LV size and two (1.7%) patients had small-sized LV. In total, five (4.3%) patients had impaired LV function,

while 111 (95.7%) patients had preserved function (Table 1).

4.3. Pulmonary arteries

Sixty-five (56%) patients had normal MPA measurement. In total, five (4.3%) patients had stenotic MPA. About 46 (39.7%) patients had dilated MPA. For RPA, 77 (66.4%) patients had normal measurement. In total, nine (7.8%) patients had stenotic RPA. About 30 (25.8%) patients had dilated RPA. For LPA, diameter was calculated for all patients apart from two (1.7%) patients who could not be

visualized. In total, 63 (54.3%) patients had normal LPA diameter. About 20 (17.2%) patients had stenotic LPA. In total, 31 (26.8%) patients had dilated LPA (Table 2, Fig. 2).

4.4. Pulmonary regurgitation

PR was graded based on regurgitation fraction as mild (<20%), moderate (20−40%), and severe [marked] (>40%) as reported by Mercer-Rosa, *et al.* (Mercer-Rosa *et al.*, 2012). In total, 16 (13.8%) patients had mild PR. About 51 (44%) patients had moderate PR. In total, 49 (42.2%) patients had severe PR (Table 3, Fig. 3).

4.5. Tricuspid regurgitation

The regurgitant volume and fraction were calculated for all patients. TR was graded as severe and nonsevere (mild or moderate) according to Medvedofsky D. *et al.* (Medvedofsky *et al.*, 2017). In total, 79 (68.1%) patients had nonsevere TR, while 12 (10.3%) had severe TR and 25 (21.6%) patients showed no TR (Table 3).

Table 2. Descriptive data of main pulmonary arteries, right pulmonary arteries, and left pulmonary arteries diameters by MRI among the studied cases.

	N = 116 (%)
MPA	
Normal	65 (56)
Stenotic	5 (4.3)
Dilated	46 (39.7)
RPA	
Normal	77 (66.4)
Dilated	30 (25.8)
Stenotic	9 (7.8)
LPA	
Normal	63 (54.3)
Dilated	31 (26.8)
Stenotic	20 (17.2)
Non visualized	2 (1.7)

Table 3. Descriptive data for important complications in post-tetralogy of Fallot repair patients.

Complications	N = 116 (%)
Pulmonary regurgitation	
No	0
Mild	16 (13.8)
Moderate	51 (44)
Severe = 3	49 (42.2)
Tricuspid regurgitation	
None	25 (21.6)
Nonsevere	79 (68.1)
Severe	12 (10.3)
Aortic root diameter	
Normal	58 (50)
Dilated	58 (50)
Aortic regurgitation	
None	98 (84.5)
Aortic regurgitation (mild)	18 (15.5)
Both aortic root dilatation and AR	9 (7.8)
Residual VSD	
None	98 (84.5)
Yes	18 (15.5)
RVOT	
Normal	87 (75)
Residual stenosis	7 (6)
Dilated	17 (14.7)
Aneurysmally dilated	5 (4.3)
Differential pulmonary flow	
Not evaluated	26 (22.4)
Evaluated	90 (77.6)
No significantly different differential pulmonary flow	51 (56.7)
Significantly different differential pulmonary flow	39 (43.3)
More flow to the right lung	36 (40)
More flow to the left lung	3 (3.3)

4.6. Aortic root diameter and AR

Measurements of the aortic root were acquired for all patients. In total, 58 (50%) patients had dilated aortic root based on Z-score. About 18 (15.5%) patients had AR, while 98 (84.5%) patients did not have AR (Table 3).

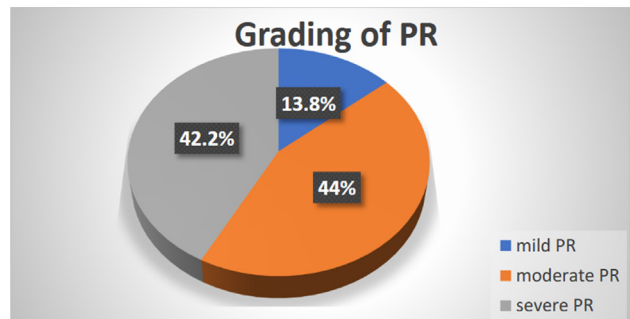Fig. 2. Diameter of left pulmonary arteries by MRI.

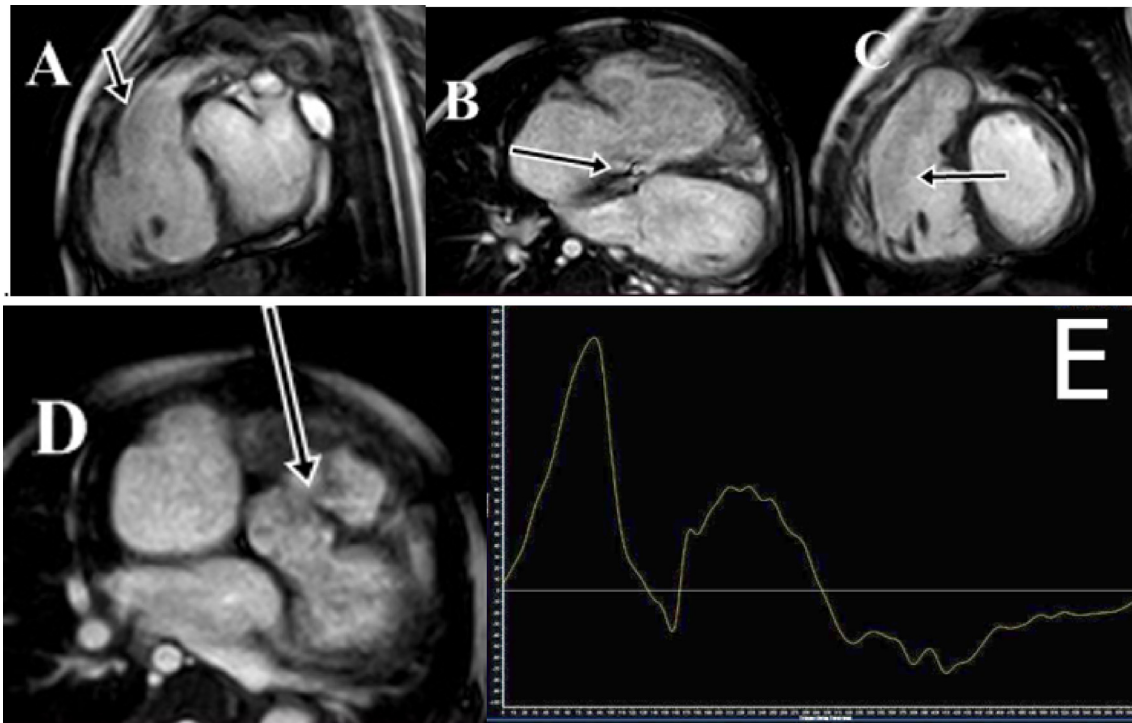Fig. 3. Grading of pulmonary regurgitation by MRI.

Fig. 4. MRI images of post-tetralogy of Fallot repair male patient aged 5 years, 9 months. (A) steady-state free precession image of right ventricle outflow tract with no residual stenosis. (B) steady-state free precession axial image showing jet of tricuspid regurge (arrow). (C) steady-state free precession short-axis image showing dilated right ventricle; end-diastolic volume index = 332.85 ml/m^2, dilated left ventricle; end-diastolic volume index = 177.23 ml/m^2 (D) steady-state free precession axial image showing ventricular septal defect patch with residual defect ~ 11 mm and jet seen through it (arrow). (E) Q-flow curve of main pulmonary arteries showing moderate pulmonary regurgitation (regurgitant fraction = 29%).

4.7. Other important complications

Eighteen (15.5%) patients had residual VSD (Fig. 4). In total, 7 patients (6%) had residual RVOT stenosis. About 17 (14.7%) patients had RVOT dilatation and five (4.3%) patients had aneurysmally dilated RVOT. Differential pulmonary flow was calculated for 90 patients, out of them, 39 patients (43.3%, 33.6% of the whole patients) had significantly different differential pulmonary flow, 36 patients had more blood flow to the right lung, while three patients had more blood flow to the left lung (Table 3, Fig. 5).

These different complications are summarized in Fig. 6.

5. Discussion

TOF is the most prevalent congenital disease of the heart characterized by RVOT stenosis, RV hypertrophy, overriding of the aorta, and VSD (Wilson et al., 2019).

The RV is a complex chamber showing semilunar shape on short-axis view, making its assessment hard by two-dimensional echocardiography. The severity of PR has a considerable effect on the decision of procedures such as pulmonary valve surgical replacement following TOF correction as well. As the operative correction of TOF has enormously improved over the past decades, the long-term survival of post-TOF correction patients has significantly increased (Van Der Ven et al., 2019).

In the current study, the right ventricle was dilated in 90.5%. This conformed with Ho et al. (2007), who reported that all cases had dilated RV.

The pulmonary arteries' diameters were measured. The most encountered abnormality was dilated MPA or its main branches as the MPA dilatation was found in 39.7% (46), dilated RPA 25.8% (30), and dilated LPA 26.8% (31) of the patients. This was disagreeing with Saraya et al. (2020), who stated that the mostly encountered complication among all of postsurgical correction of variable complex congenital heart disease patients was branch pulmonary stenosis (39%). Considering that the later study was not specific for post-TOF repair patients. Yet, when comparing the current results with Saraya et al. (2020) study for TOF cases only, a good agreement was found between both studies regarding the percentages of branch pulmonary stenosis among patients of TOF, which were 18% and 12.6%, respectively.
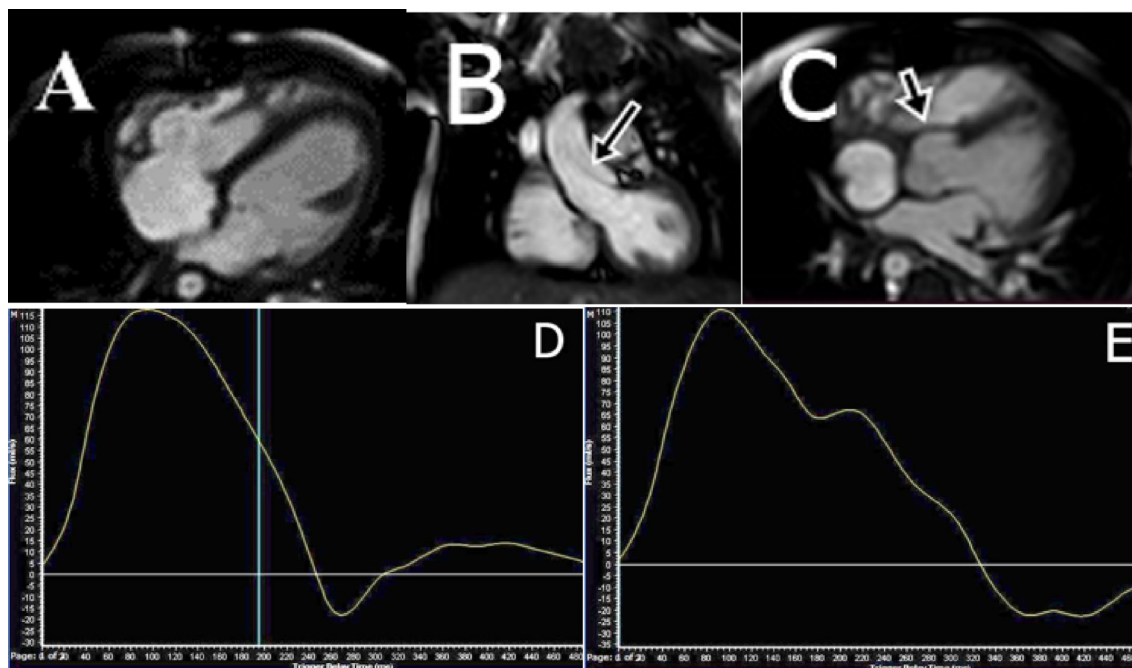
Fig. 5. MRI images of post-tetralogy of Fallot repair male patient aged 2 years. (A) steady-state free precession axial image showing dilated left ventricle (end-diastolic volume index = 95 ml/m^2) and dilated mildly hypertrophied right ventricle (end-diastolic volume index = 92 ml/m^2). (B) Steady-state free precession Left ventricle outflow tract image showing dilated aortic root (arrow). (C) Steady-state free precession axial image showing intact ventricular septal defect patch with no residual defect (arrow). (D) Q-flow curve of the ascending aorta showing mild aortic regurgitation (regurgitation fraction 3%). (E) Q-flow curve of main pulmonary arteries showing mild pulmonary regurgitation (regurgitation fraction 15%).

As regards PR, there was excellent concordance between this study and Mercer-Rosa et al. (2012) in the prevalence of severe PR patients (42.2% of the patients had severe PR in the current study), and 40% in Mercer-Rosa et al. (2012) and relative concordance with Saraya et al. (2020), where the prevalence of severe PR was 55%.

The diameter of the aortic root was measured and interpreted based on Z-scores. About 58 (50%) patients had aortic root dilatation. This came in disagreement with Cruz et al. (2018), who disclosed the prevalence of dilatation of the aortic root among the studied cases at the levels of ascending aorta and sinus of Valsalva to be 24% and 29%, respectively.

Eighteen (15.5%) patients demonstrated mild aortic regurgitation. This agreed with Niwa et al. (2002), who observed the prevalence of AR among TOF cases to be 15%. This also came in relative accordance with Mongeon FP et al. (Mongeon et al., 2013), who disclosed AR prevalence among post-TOF correction patients to be 13.6%.

Out of these 18 patients, nine patients had both dilatation of the aortic root and AR constituting 15.5% of 58 patients with dilated aortic root and 7.8% of all patients of the study. This conforms with Grotenhuis, H. B et al. (Grotenhuis et al., 2018) who observed that

AR is not common in the pediatric TOF patients and does not represent an important morbidity and this could be due to young age at correction of TOF, also, as both studies were done on pediatrics, progression of this morbidity requires lifelong monitoring and follow-up for accurate evaluation.

The percentage of RVOT dilatation was 14.7%, 17. In total, five (4.3%) patients had aneurysmal dilatation of the RVOT staunchly opposing to Davlouros Periklis et al. (Davlouros Periklis et al., 2002). As the latter mentioned common prevalence of RVOT aneurysm dilatation (56.9%). This great discordance could be illustrated by the variance in the age of the study population. The current study involved patients in pediatric age group, while Davlouros Periklis et al. (Davlouros Periklis et al., 2002) involved adult population on long-term follow-up.

In the current study, the prevalence of recurrent or residual RVOT narrowing was about 6% (7 patients). This was in discordance with Ho et al. (2007), who reported that the percentage of recurrent or residual RVOT stenosis was ~42%.

The estimated prevalence of residual VSD among the study population was 15.5% (18 patients). This was in relative harmony with Ho et al. (2007), who reported that the percentage of residual VSD was about 10%.

Reporting checklist

First,
segmental analysis
especially:
- Situs.
- Concordance.
-Aorto-pulmonary relation

Then, evaluation of the cardiac
chambers

RV and LV for both
size and function

RA and LA
dilated or not

Valvular
analysis

Pulmonary

Tricuspid

Aortic

Mitral

Evaluate the
major arteries

Aorta

Pulmonary
artery and its
branches

Address the most common
complications in order

PR

RV size and function deterioration

Pulmonary arteries dilatation/stenosis and
differential pulmonary flow

Aortic root dilatation/AR

TR

Other complications:
- RVOT dilatation/significant stenosis.
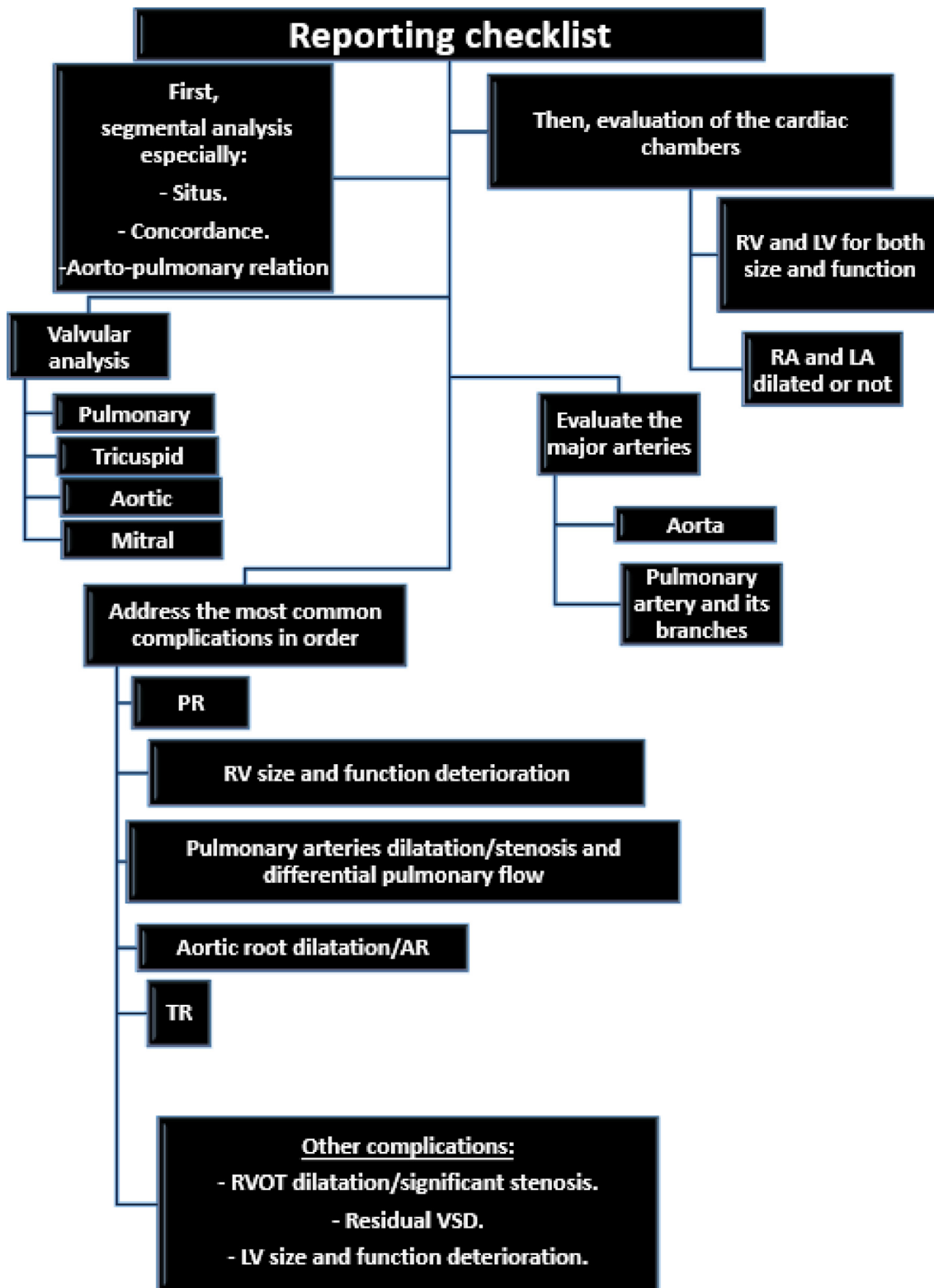- Residual VSD.
- LV size and function deterioration.

Fig. 6. Checklist for summarizing complications that should be evaluated on post-tetralogy of Fallot surgical repair patients by cardiac magnetic resonance imaging.

In this study, differential pulmonary flow was measured for 90 patients, out of them, 39 (43.3%) patients had significantly different differential pulmonary flow, 36 (40%) patients had more blood flow to the right lung, while three (3.3%) patients only had more blood flow to the left lung. This could be utilized to estimate the functional significance of branch pulmonary artery stenosis and guide to management (Sridharan et al., 2006).

Eventually severe PR can lead to variable grave complications such as RV dysfunction or arrythmia and may require pulmonary valve replacement, so, it should undergo routing follow-up clinically and with echocardiography and CMRI. The timing of this procedure is very important. Therefore, a careful interpretation of the degree of PR and PA has a direct impact on the decision of the management (Vaujois et al., 2016).

So, routine follow-up of surgically corrected TOF patients with cardiac MRI with a timely plan based on the patients' status is important for evaluation of the previously mentioned items that is mandatory for early detection of possible encountered complications to allow for early intervention and correction, which leads to improved prognosis, quality of life, and decrease in morbidity and mortality.

5.1. Limitations

(1) The study was performed without contrast administration. The use of gadolinium is important as many cases of post-TOF repair could have myocardial scarring detected as delayed myocardial contrast enhancement following operation as discussed by Cochet et al. (2019).
(2) This study was a single-center study, future multicenter study with long-term monitoring would be more informative.

5.2. Conclusions

Magnetic resonance imaging is critical for evaluation of post-TOF repair patients and possible complications. CMRI is accurate in quantifying PR, RV size, and function and evaluating other possible important complications related to RVOT, pulmonary arterial diameters and differential flow, VSD closure, and LV function and size as well.

Conflicts of interest

There are no conflicts of interest.

References

Buechel, E.V., Kaiser, T., Jackson, C., et al., 2009. Normal right- and left ventricular volumes and myocardial mass in children measured by steady state free precession cardiovascular magnetic resonance. J. Cardiovasc. Magn. Reson. 11, 1−9.

Cantinotti, M., Giordano, R., Scalese, M., et al., 2017. Nomograms for two-dimensional echocardiography derived valvular and arterial dimensions in Caucasian children. J. Cardiol. 69, 208−215.

Cochet, H., Iriart, X., Allain-Nicolaï, A., et al., 2019. Focal scar and diffuse myocardial fibrosis are independent imaging markers in repaired tetralogy of Fallot. Eur Heart J- Cardiovasc Imaging 20, 990−1003.

Cruz, C., Pinho, T., Ribeiro, V., et al., 2018. Aortic dilatation after tetralogy of Fallot repair: A ghost from the past or a problem in the future? Rev. Port. Cardiol. 37, 549−557.

Dahiya, A., Sharma, R., Joshi, P., 2022. Unusual presentation of RVOT aneurysm. IHJ Cardiovascular Case Reports (CVCR) 6, 53−55.

Davlouros Periklis, A., Kilner Philip, J., Hornung Tim, S., et al., 2002. Right ventricular function in adults with repaired tetralogy of Fallot assessed with cardiovascular magnetic resonance imaging. J. Am. Coll. Cardiol. 40, 2044−2052.

Geva, T., 2014. Repaired tetralogy of Fallot: the roles of cardiovascular magnetic resonance in evaluating pathophysiology and for pulmonary valve replacement decision support. J. Cardiovasc. Magn. Reson. 13, 9.

Grotenhuis, H.B., Dallaire, F., Verpalen, I.M., et al., 2018. Aortic root dilatation and aortic-related complications in children after tetralogy of Fallot repair. Circ: Cardiovasc Imaging 11, 007611.

Haggerty, C.M., Suever, J.D., Pulenthiran, A., et al., 2017. Association between left ventricular mechanics and diffuse myocardial fibrosis in patients with repaired tetralogy of Fallot: a cross-sectional study. J. Cardiovasc. Magn. Reson. 19, 100.

Ho, K.W., Tan, R.S., Wong, K.Y., et al., 2007. Late complications following tetralogy of Fallot repair: the need for long-term follow-up. Ann. Acad. Med. Singapore 36, 947.

Hysinger, E.B., Higano, N.S., Critser, P.J., et al., 2022. Imaging in neonatal respiratory disease. Paediatr. Respir. Rev. 43, 44−52.

Kalyan, S., Das, S., Raj, V., 2021. Pre-and Postoperative Imaging in Tetralogy of Fallot. CT and MRI in Congenital Heart. Diseases 315−330.

Medvedofsky, D., Jiménez, J.L., Addetia, K., et al., 2017. Multiparametric quantification of tricuspid regurgitation using cardiovascular magnetic resonance: a comparison to echocardiography. Eur. J. Radiol. 86, 213−220.

Mercer-Rosa, L., Yang, W., Kutty, S., 2012. Quantifying pulmonary regurgitation and right ventricular function in surgically repaired tetralogy of Fallot: a comparative analysis of echocardiography and magnetic resonance imaging. Circulation: Cardiovascular Imaging 5, 637−643.

Mongeon, F.P., Gurvitz, M.Z., Broberg, C.S., et al., 2013. Aortic root dilatation in adults with surgically repaired tetralogy of fallot: a multicenter cross-sectional study. Circulation 127, 172−179.

Niwa, K., Siu, S.C., Webb, G.D., et al., 2002. Progressive aortic root dilatation in adults late after repair of tetralogy of Fallot. Circulation 106, 1374−1378.

Renella, P., Aboulhosn, J., Lohan, D.G., et al., 2010. Two-dimensional and Doppler echocardiography reliably predict severe pulmonary regurgitation as quantified by cardiac magnetic resonance. J. Am. Soc. Echocardiogr. 23, 880−886.

Saraya, S., Woodard, P., Bhalla, S., et al., 2020. Cardiac MRI in evaluation of post-operative congenital heart disease and complications. J Radiol Nucl Med 51, 1—12.

Schicchi, N., Secinaro, A., Muscogiuri, G., et al., 2016. Multicenter review: role of cardiovascular magnetic resonance in diagnostic evaluation, pre-procedural planning and follow-up for patients with congenital heart disease. La radiologia medica 121, 342—351.

Sridharan, S., Derrick, G., Deanfield, J., et al., 2006. Assessment of differential branch pulmonary blood flow: a comparative study of phase contrast magnetic resonance imaging and radionuclide lung perfusion imaging. Heart 92, 963—968.

Valente, A.M., Cook, S., Festa, P., et al., 2014. Multimodality imaging guidelines for patients with repaired tetralogy of Fallot: a report from the American Society of Echocardiography: developed in collaboration with the Society for Cardiovascular Magnetic Resonance and the Society for Pediatric Radiology. J. Am. Soc. Echocardiogr. 27, 111—141.

Van Der Ven, J.P.G., Van Den Bosch, E., Bogers, A.J., et al., 2019. Current outcomes and treatment of tetralogy of Fallot. F1000Research 8, F1000 Faculty Rev-1530.

Vaujois, L., Gorincour, G., Alison, M., et al., 2016. Imaging of postoperative tetralogy of Fallot repair. Diagn Interv Imaging 97, 549—560.

Wilson, R., Ross, O., Griksaitis, M.J., 2019. Tetralogy of Fallot. BJA education 19, 362—369.

Woodard, P.K., Ho, V.B., Akers, S.R., et al., 2017. ACR Appropriateness Criteria((R)) Known or Suspected Congenital Heart Disease in the Adult. J. Am. Coll. Radiol. 14, S166—S176.